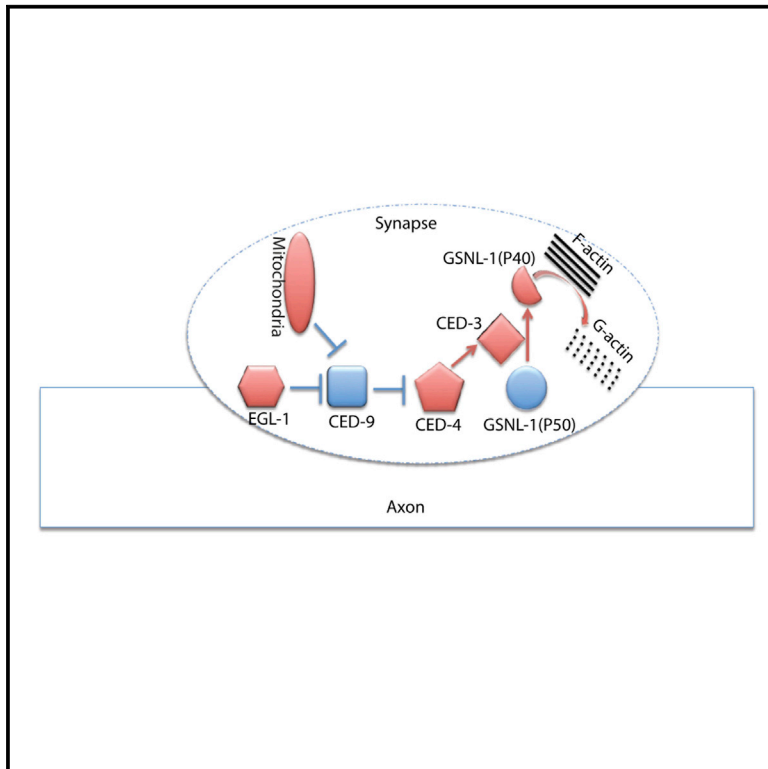


The Cell Death Pathway Regulates Synapse Elimination through Cleavage of Gelsolin in *Caenorhabditis elegans* Neurons

Graphical Abstract



Authors

Lingfeng Meng, Ben Mulcahy, Steven J. Cook, ..., Airong Wan, Yishi Jin, Dong Yan

Correspondence

dong.yan@duke.edu

In Brief

Meng et al. find that activation of the cell death pathway in *C. elegans* neurons contributes to selective elimination of synapses through disassembly of the actin filament network.

Highlights

- The cell death (CED) pathway is required for synapse elimination
- Axonal mitochondria regulate synapse elimination through the CED pathway in vivo
- GSNL-1 acts downstream of the CED pathway in synapse elimination
- Cleavage of GSNL-1 by CED-3 induces F-actin disassembly and synapse elimination



The Cell Death Pathway Regulates Synapse Elimination through Cleavage of Gelsolin in *Caenorhabditis elegans* Neurons

Lingfeng Meng,¹ Ben Mulcahy,² Steven J. Cook,³ Marianna Neubauer,⁴ Airong Wan,¹ Yishi Jin,^{5,6,7} and Dong Yan^{1,8,*}

¹Department of Molecular Genetics and Microbiology, Duke University Medical Center, Research Drive, Durham, NC 27710, USA

²Lunenfeld-Tanenbaum Research Institute, Toronto, ON M5G 1X5, Canada

³Dominick P. Purpura Department of Neuroscience, Albert Einstein College of Medicine, Bronx, NY 10461, USA

⁴Department of Physics and Center for Brain Science, Harvard University, Cambridge, MA 02138, USA

⁵Neurobiology Section, Division of Biological Sciences, University of California, San Diego, La Jolla, CA 92093, USA

⁶Department of Cellular and Molecular Medicine, School of Medicine, University of California, San Diego, La Jolla, CA 92093, USA

⁷Howard Hughes Medical Institute, Chevy Chase, MD 20815, USA

⁸Department of Neurobiology and Duke Institute for Brain Sciences, Duke University Medical Center, Research Drive, Durham, NC 27710, USA

*Correspondence: dong.yan@duke.edu

<http://dx.doi.org/10.1016/j.celrep.2015.05.031>

This is an open access article under the CC BY-NC-ND license (<http://creativecommons.org/licenses/by-nc-nd/4.0/>).

SUMMARY

Synapse elimination occurs in development, plasticity, and disease. Although the importance of synapse elimination has been documented in many studies, the molecular mechanisms underlying this process are unclear. Here, using the development of *C. elegans* RME neurons as a model, we have uncovered a function for the apoptosis pathway in synapse elimination. We find that the conserved apoptotic cell death (CED) pathway and axonal mitochondria are required for the elimination of transiently formed clusters of presynaptic components in RME neurons. This function of the CED pathway involves the activation of the actin-filament-severing protein, GSNL-1. Furthermore, we show that caspase CED-3 cleaves GSNL-1 at a conserved C-terminal region and that the cleaved active form of GSNL-1 promotes its actin-severing ability. Our data suggest that activation of the CED pathway contributes to selective elimination of synapses through disassembly of the actin filament network.

INTRODUCTION

The formation of precise connections between neurons is an essential step of brain development, starting from development of axons and dendrites and followed by formation and elimination of synapses. In early developmental stages, an excessive number of synapses are formed between neurons, and a portion of them subsequently are eliminated during the maturation of neural circuits to ensure the formation of correct connections (Huttenlocher et al., 1982; Kamiyama et al., 2006; Keller-Peck et al., 2001; Rosenthal and Taraskevich, 1977; Walsh and Lichtman, 2003; Zuo et al., 2005a). Although neuronal activity has

been shown to play critical roles in synapse elimination, the molecular mechanisms of synapse elimination are still largely unknown (Flavell and Greenberg, 2008; Kakizawa et al., 2000; Nelson et al., 1993; Rabacchi et al., 1992; Thompson, 1983, 1985; Zuo et al., 2005b).

The programmed-apoptosis cell death (CED) pathway removes extra cells during development and eliminates unhealthy cells in diseases (Hyman and Yuan, 2012). More and more studies show that the apoptosis pathway also plays important roles in neural development and function. In *Drosophila melanogaster* and cultured hippocampal neurons, local activation of caspases promotes dendritic pruning (Ertürk et al., 2014; Kuo et al., 2006; Williams et al., 2006). In olfactory sensory neurons and retinal ganglion cells, the apoptosis pathway regulates axon guidance through cleavage of membrane-anchored semaphorin and MAP kinases (Campbell and Holt, 2003; Ohsawa et al., 2010). Caspases also are involved in learning and memory in zebra finch and mice (Huesmann and Clayton, 2006; Jiao and Li, 2011; Li et al., 2010). In long-term depression (LTD), local activation of caspase-3 mediates AMPA receptor internalization through cleavage of Akt (Li et al., 2010). Recently, several studies shed light on the function of the apoptosis pathway in synapse elimination. Local activation of caspase-3 by mitochondrial dysfunction induces pruning of dendritic spines in cultured hippocampal neurons, and the spine density is increased in caspase-3 knockout mice (Ertürk et al., 2014). At the neuromuscular junction (NMJ), the activation of caspase-3 cleaves Dishevelled to promote the elimination of postsynaptic structures (Wang et al., 2014). However, Dishevelled appears to play moderate roles in other synapses (Luo et al., 2002), suggesting refinement of synapse connections in different types of synapses may involve other caspase targets. The elimination of synapses includes pruning of both presynaptic and postsynaptic structures. While many efforts have led to the dissection of the signaling pathways in regulation of postsynaptic structures, very few studies have focused on refinement of presynaptic structures. Since presynaptic boutons can develop without postsynaptic

signals (Murthy and De Camilli, 2003), it is reasonable to speculate that the elimination of presynaptic structures is an active process rather than the consequence of elimination of postsynaptic structures. Therefore, it is important to understand the regulatory mechanisms of the elimination of presynaptic structures.

The filamentous actin (F-actin) is enriched at growth cones and synaptic regions, and regulation of actin dynamics is important for neural development (Luo, 2002). Polymerization and de-polymerization of actin filaments, upon stimulation by different guidance cues, regulates the formation and retraction of filopodia and lamellipodia as axons grow toward developmental targets (O'Donnell et al., 2009). In cultured hippocampal neurons, de-polymerization of F-actin in young synapses by latrunculin A triggers synapse loss (Zhang and Benson, 2001). F-actin assembly is also important for clustering synaptic vesicles around the active zone (Doussau and Augustine, 2000; Murthy and De Camilli, 2003). In addition, the Rho GTPase family, including RhoA, Rac1, and Cdc42, modulates actin dynamics to instruct axonal growth and spine formation, growth, maintenance, and retraction (Luo, 2002). In *C. elegans*, F-actin can bind with the presynaptic active zone proteins SYD-1 and SYD-2 through an adaptor protein NAB-1 (neurabin) to promote presynaptic assembly and axonal branching (Chia et al., 2012, 2014).

The actin-severing gelsolin/villin superfamily is a key regulator of actin filament assembly and disassembly. Most of the gelsolin family proteins are cytoplasmic proteins and are regulated by calcium. Gelsolin proteins bind to the barbed ends of actin filaments to prevent monomer exchange and sever existing filaments (Silacci et al., 2004). In *C. elegans* there are three gelsolin-related proteins: *gsnl-1*, *viln-1*, and *fli-1*, among which *gsnl-1* is the most characterized. Unlike the conventional gelsolin proteins that have either three or six gelsolin-like domains, GSNL-1 has four gelsolin-like domains (Klaavuniemi et al., 2008). In vitro studies show that GSNL-1 can sever actin filaments and caps the barbed end in a calcium-dependent manner, similar to that of conventional gelsolin proteins (Klaavuniemi et al., 2008). However, the function of *C. elegans* gelsolin proteins in neural development remains unclear.

Here we show how the apoptosis pathway regulates activation of the gelsolin-like protein, GSNL-1, to instruct actin de-polymerization and to control the elimination of transient clusters of presynaptic components. We used a pair of *C. elegans* head motor neurons, RME dorsal (RMED) and ventral (RMEV) neurons, as our model. In an unbiased genetic screen, we uncovered a loss-of-function allele of *ced-3* with strong defects in the localization of presynaptic components. CED-3 is the major apoptotic caspase in *C. elegans* and functional homolog of mammalian caspase 3 (Hyman and Yuan, 2012; Yuan et al., 1993). We also found that four core components of the *C. elegans* apoptosis pathway are all required for the elimination of transient presynaptic components, and that axonal mitochondria are important for activating the CED pathway in this process. In the same genetic screen, we identified a loss-of-function allele of *gsnl-1* with similar phenotypes as *ced-3(lf)*. Further studies showed that CED-3 cleaves GSNL-1 at a C-terminal conserved site to promote its F-actin-severing ability and to promote disassembly of presynaptic components at improper locations. Therefore, our

study has revealed the function of axonal mitochondria and the apoptosis pathway in the elimination of presynaptic components in vivo, and we have identified a gelsolin protein as a downstream target of the caspase in elimination of presynaptic components. The conservation of the CED-3 cleavage site in GSNL-1 indicates this regulation may be a conserved mechanism for synapse elimination in other organisms.

RESULTS

RME Neurons Transiently Accumulate Presynaptic Components in Dendritic Neurites

C. elegans head movement is controlled by four GABAergic RME neurons: RME dorsal (D), RME left (L), RME right (R), and RME ventral (V) (White et al., 1986). The somas of RME neurons are located close to the nerve ring, and their axons grow as a ring-shaped bundle surrounding the pharyngeal region where they form en passant synapses with a subset of head muscles. RMED and RMEV extend two posterior dendritic neurites along the dorsal and ventral cords (Figures 1A and 1B). Four RME neurons migrate to their final position during embryo development, but the development of those dorsal and ventral (D/V) neurites occurs after hatching, and their function remains unknown (Figure 1B). Using synaptobrevin-GFP (SNB-1-GFP) to label presynaptic vesicles in RME neurons, we observed that at early larval stage (L1), in addition to their normal accumulation at the nerve ring, clusters of SNB-1-GFP also misaccumulated at the end of D/V neurites and continued to add until late L1 stage (Figures 1C and 1D). By L2 stage the misaccumulated SNB-1-GFP puncta in D/V neurites started pruning, and they were below detection in L3 or later-stage animals (Figure 1C).

To verify that these fluorescent puncta might contain other presynaptic components, we further examined the localization of presynaptic active zone protein SYD-2/Liprin- α in different developmental stages (Yeh et al., 2005). As shown in Figures 1E and 1F, SYD-2/Liprin- α formed puncta in D/V neurites at L1 stage, and those puncta were completely eliminated before L3 stage similar to those of the SNB-1-GFP marker. Using another marker for synaptic vesicles, RAB-3-mCherry, we also observed the presence of fluorescent punctate signals in L1 D/V neurites, and RAB-3-mCherry signal was completely co-localized with presynaptic active zone marker SYD-2 (Figures S1A and S1B). To further verify our observation, we tested whether the formation of SNB-1-GFP puncta in RMED/V neurites required *syd-2* and *unc-104*, two molecules necessary for the formation of presynaptic vesicle clusters (Hall and Hedgecock, 1991; Zhen and Jin, 1999). As shown in Figure 1G, SNB-1-GFP puncta in D/V neurites were undetectable in L1 animals of loss-of-function mutants for *syd-2* and *unc-104*. These analyses indicate that RMED/V neurons may transiently accumulate presynaptic components in their D/V neurites during development.

To assess if some of the transient presynaptic clusters formed morphological synapses, we reconstructed the D/V neurite of RMED and RMEV in a wild-type L1 animal (14 hr post-hatching) by serial section transmission electron microscopy (TEM). RMED and RMEV were identified based on their cell body locations and

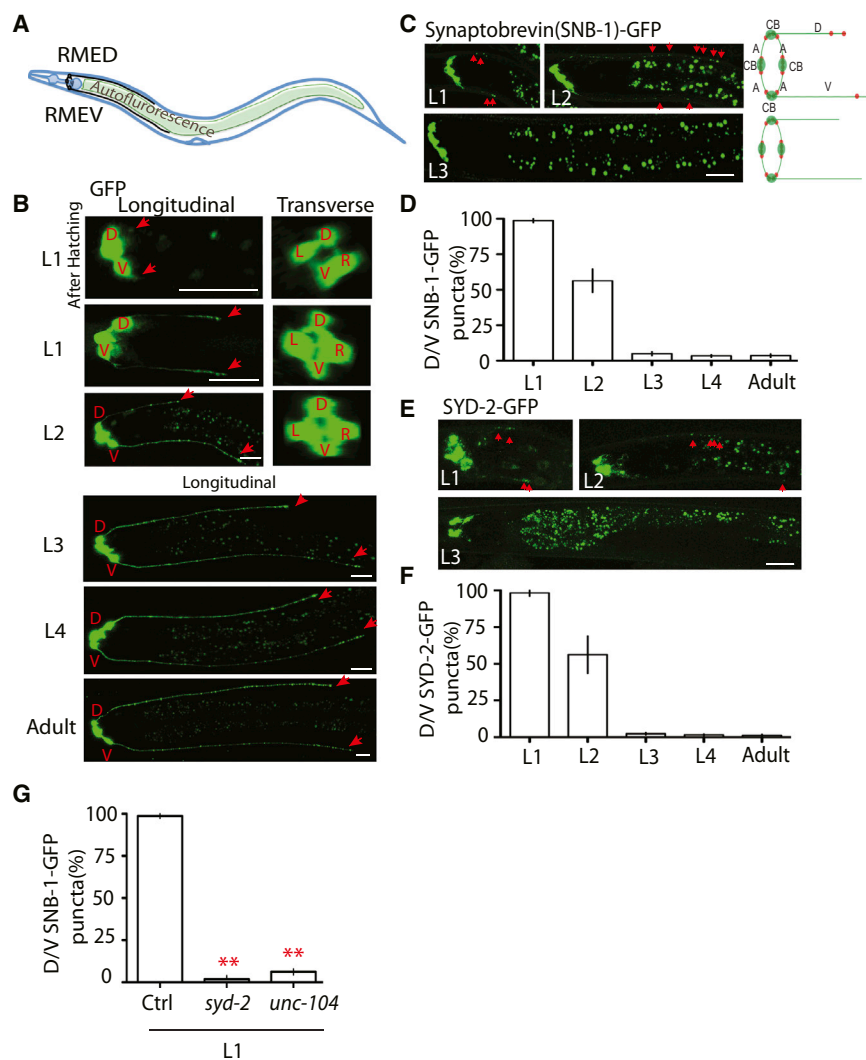


Figure 1. RME and RMEV Neurons Form Transient Clusters of Presynaptic Components at Dendritic D/V Neurites during Larval Development

(A) The morphology of RME neurons. RME neurons (black) locate in the head region of *C. elegans*, and RME axons form a ring-shaped bundle at the nerve ring region. RME and RMEV grow two posterior neurites along the D/V cords. When imaging RME neurons, the gut autofluorescence is often seen between the D and V cords (B, C, and E).

(B) The development of RME D/V neurites visualized by a marker expressing GFP in RME neurons (*Punc-25::GFP*). The four RME neurons migrated to their final position before hatching, but the development of D/V neurites occurred after hatching. Red arrows label the end of D/V neurites. D, RME; V, RMEV; L, RME; R, RME.

(C–F) RME D/V neurons form transient synapses at early developmental stages. At the first larval (L1) stage, synaptic vesicles and synaptic active zones are clustered at D/V neurites. No synaptic vesicle and synaptic active zone puncta were observed in L3 worms. Representative images and schematics show the localization of synaptic vesicle puncta (Synaptobrevin [SNB-1]-GFP, C) and synaptic active zone puncta (SYD-2-GFP, E) in RME neurons. CB, cell bodies; A, axons; D/V, dorsal/ventral neurites; red dot, synaptic puncta. Red arrowheads highlight the transient clusters of presynaptic components. (D and F) Quantification of the percentage of animals with D/V puncta.

(G) Quantification data show that loss of function in *syd-2* and *unc-104* causes the absence of SNB-1-GFP puncta in D/V neurites of L1 animals. Experiments were performed at least three times, with $n \geq 80$ animals each time.

Data are shown as mean \pm SD. Student's t test, ** $p < 0.01$. Scale bar, 10 μ m.

neurite trajectories. We traced the entire D and V neurites from the cell bodies of each neuron. They both showed periodic swellings (Figures S2A and S2B). Multiple cellular organelles, including mitochondria, microtubules, and vesicular structures, were present in these swellings (Figure S2A). Figure S2B shows a complete series of EM images for one such swelling. However, we did not detect mature presynaptic structures in the swelling regions (Figures S2A and S2B). As a control, we observed the classic mature chemical synaptic structures with synaptic vesicle clusters and active zones in the neighboring DA and DB motor neuron axons. These results suggest that, while both RME D/V branches contain swelling structures enriched with vesicular components at the L1 stage, the fluorescent puncta from our reporters likely represent mis-localized or improperly formed clusters of presynaptic components during development. Since the formation and elimination of the fluorescent puncta happened at the same developmental stage in all animals, the development of RME D/V neurites is an appropriate system to study the molecular mechanisms of elimination of synaptic components.

The CED Pathway Regulates the Elimination of Presynaptic Components

To understand what controls the elimination of presynaptic components in RME neurons, we conducted a genetic screen and isolated mutants that retained SNB-1-GFP puncta in D/V neurites at the adult stage. One mutant uncovered in this screen, *ju1056*, showed synaptic vesicle cluster elimination defects in over 90% of animals (Figure 2A). *ju1056* was mapped to chromosome IV, tightly linked to *unc-30*. After testing several candidate genes, we found that *ju1056* failed to complement the loss-of-function (*lf*) allele of the *C. elegans* apoptotic gene *ced-3* (*n717*). Sequencing results showed that *ju1056* causes a glycine to arginine point mutation in the conserved caspase domain of CED-3 (Figure S1C; Table S1). Besides SNB-1-GFP phenotypes, we also noticed that about 30%–40% of animals had additional neurons in the head region (data not shown). To confirm the SNB-1-GFP elimination phenotype was not a secondary effect due to change of neuron numbers, we expressed *ced-3* cDNA at a low concentration only in RME neurons and quantified its rescue ability. As shown in Figure 2B, expression of *ced-3* in

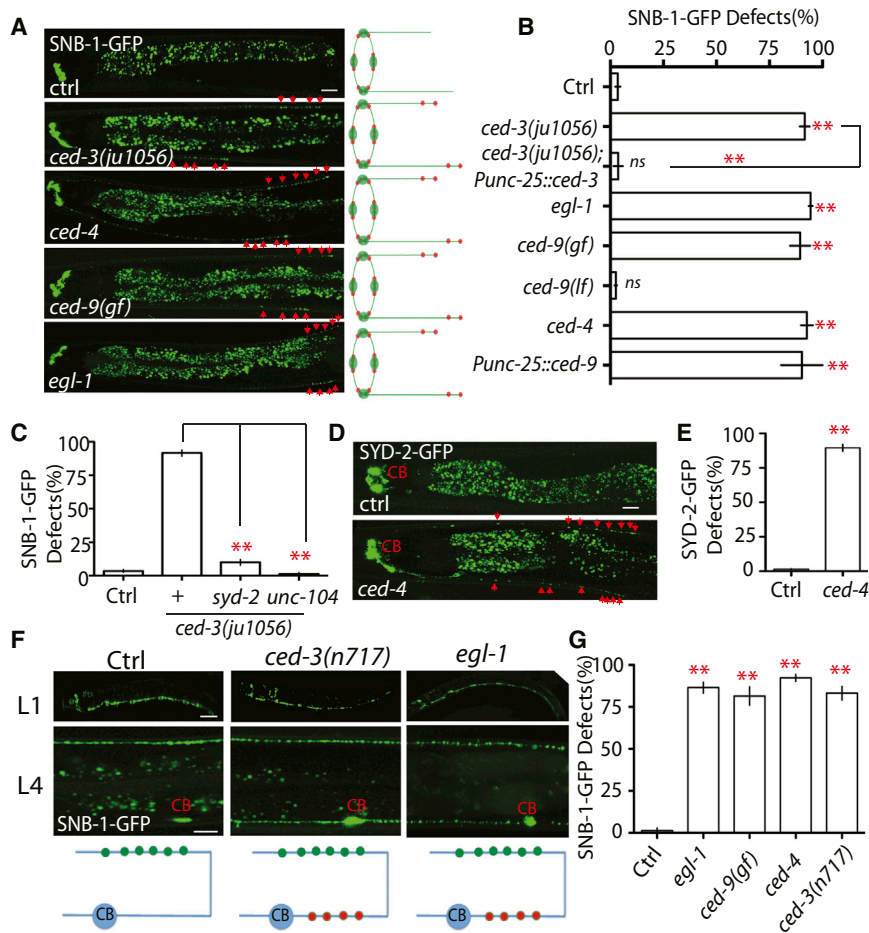


Figure 2. The Apoptotic CED Pathway Is Required for the Elimination of Presynaptic Components

(A and B) Loss of function in the CED pathway prevents the elimination of presynaptic components. (A) Images and schematics of the localization of synaptic vesicle puncta in wild-type and mutant animals. (B) Quantification of SNB-1-GFP elimination defects (percentage animals) in different genotypes. *Punc-25* promoter was used to express genes in RME neurons; *unc-30(ju32)* animals were used as background to eliminate *unc-25* expression in the D neurons. The strain information is listed in Tables S1 and S2.

(C) Quantification data show that loss of function in *syd-2* and *unc-104* suppresses SNB-1-GFP elimination defects in *ced-3(lf)* animals.

(D and E) Loss of function in *ced-4* suppressed the elimination of presynaptic active zones. (D) Images show the localization of active zone puncta (*Punc-25::SYD-2-GFP*). (E) Quantification of active zone elimination defects is shown.

(F and G) The CED pathway regulates synapse elimination in DD motor neurons. (F) Images and schematics show the localization of synaptic puncta (*Pflp-13-SNB-1::GFP/juls137*) in wild-type, *ced-3(lf)*, and *egl-1(lf)* animals at L1 and L4 stages. CB, cell bodies; green dot, new synapses at the dorsal cord; red dot, synapses at the ventral cord. (G) Graph shows the quantification data of DD motor neuron synapse elimination defects in L4 animals.

In (B), (E), and (G), experiments were performed at least three times, with $n \geq 80$ animals each time. For transgenic animals, the results shown here are generated from at least three independent lines. Data are shown as mean \pm SD. Student's *t* test, ** $p < 0.01$; ns, no significant difference. Scale bar, 10 μ m. See also Figure S1.

RME neurons fully rescued SNB-1-GFP elimination defects in *ced-3(lf)*, suggesting *ced-3* promotes the elimination of presynaptic components through regulation of signals in RME neurons rather than through affecting cells surrounding RME neurons.

CED-3 is one of the four core components of the *C. elegans* apoptotic pathway that also includes the BH3 domain protein EGL-1, the anti-apoptotic Bcl-2 homolog CED-9, and the Apaf-1-like protein CED-4 (Hyman and Yuan, 2012). To test whether other members of this pathway are involved in the elimination of presynaptic components, we quantified SNB-1-GFP defects in mutants altering functions of these proteins. We found that loss of function in pro-apoptotic genes, *egl-1* and *ced-4*, and gain of function in the anti-apoptotic gene *ced-9* induced elimination defects to a similar degree as *ced-3(lf)* mutants, while loss of function in *ced-9* did not show any obvious defects (Figures 2A and 2B). Further evidence showed that the formation of the SNB-1-GFP puncta in D/V neurites depended on key regulators of synapse formation: *syd-2* and *unc-104* (Figure 2C). To evaluate whether the sizes of these SNB-1-GFP puncta were similar to those seen in normal synapses, we compared SNB-1-GFP puncta in RMED neurites with nearby synapses from DD motor neurons. We found that in all CED and other mutants described in this study, at the end

of RMED neurites, the SNB-1-GFP puncta were similar in size and fluorescence intensity to those in DD synapses (Figure S1D). Quantification data showed none of these mutants altered the overall expression level of SNB-1-GFP in RME neurons (Figure S1E). Blockage of the CED pathway by loss of function in *ced-4* also prevented the elimination of the presynaptic active zone marker SYD-2-GFP (Figures 2D and 2E). These results demonstrate that the activation of the CED pathway is required for the elimination of synaptic components during development. To further support this conclusion, we suppressed the CED pathway by overexpression of the anti-apoptotic gene *ced-9* cDNA in RME neurons. Unlike in CED mutants, we did not observe any additional neurons in CED-9-overexpressing transgenic lines (total six lines), but all these lines showed similar phenotypes to *ced-3(lf)* mutants, supporting the finding that the elimination defects of CED mutants are due to inactivation of the CED pathway in RME neurons during development (Figure 2B).

Elimination of synapses has been observed previously in DD motor neurons. DD neurons undergo remodeling during larval development, including elimination of transient synapses in the ventral cord and establishment of new synaptic connections in the dorsal cord (Hallam and Jin, 1998; White et al., 1978, 1986).

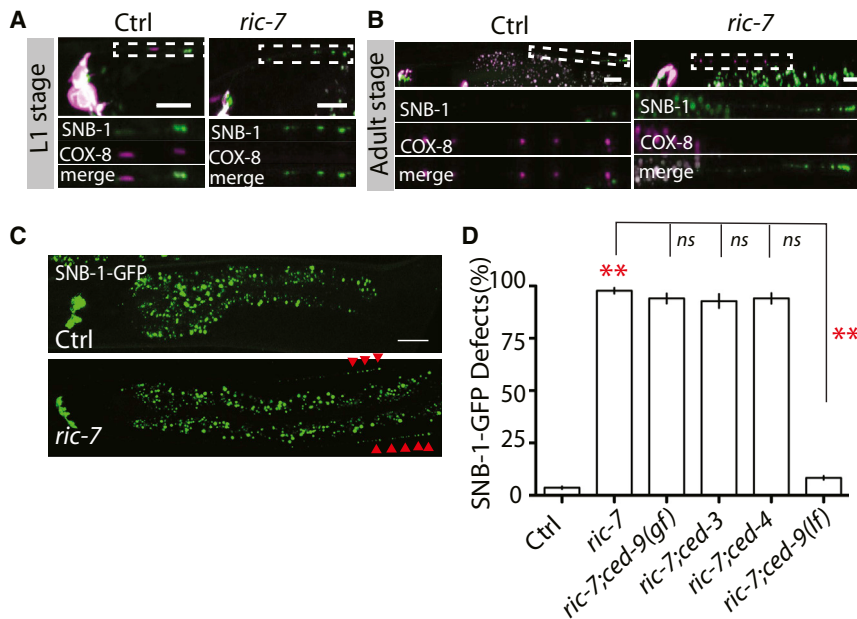


Figure 3. Axonal Mitochondria Are Required for Synapse Elimination in RME Neurons

(A) Mitochondria, labeled by COX-8-Crimson, are co-localized with SNB-1-GFP in D/V neurites of L1 animals, and this synaptic localization requires *ric-7*. (B) *ric-7* plays an important role in D/V neurite localization of mitochondria in adult animals.

(C and D) Images (C) and quantification (D) show that loss of function in *ric-7* prevents synapse elimination through CED-9. Experiments were performed at least three times, with $n \geq 80$ animals each time.

Data are shown as mean \pm SD. Student's t test, ** $p < 0.01$. Scale bar, 10 μ m. See also Figures S2 and S3.

at synaptic regions or very close to synapses in RME/D/V neurites and DD motor neurons (Figures 2A and S3A), raising the possibility that mitochondria also may regulate synapse elimination in *C. elegans*. To test this hypothesis, we investigated the development of RME

DD neurons complete remodeling at L2 stage, eliminating all ventral synapses and forming dorsal synapses. Using a marker labeling DD neuron synapses, we found that the formation of dorsal synapses appeared to be normal in all CED mutants, but the elimination of ventral synapses was suppressed (Figure 2F). About 80% of the CED mutant animals showed visible synapses in the ventral cord at L4 stage (Figures 2F and 2G). But, unlike in RME neurons, the synapse elimination defects dramatically decreased after L4 stage and were undetectable in 2-day-old adults (Figure S2C), suggesting other pathways may act in parallel with the CED pathway in DD motor neurons. Nevertheless, these results show that the activation of the CED pathway is likely a common mechanism for synapse elimination in *C. elegans*. By examining DD neurons, we were also able to conclude that the observed CED mutant phenotypes were due to defects in synapse elimination, but not defects in neuronal polarity. In L1 animals, DD neurons extend neurites in both dorsal and ventral cords, but only establish synaptic connections in the ventral cord (Hallam and Jin, 1998). If the CED pathway were required for the establishment of neuronal polarity, we would expect to see synapses in both dorsal and ventral cords in CED mutants. But we did not observe any synaptic puncta in the D cord of L1 mutant animals (Figure 2F), supporting the finding that the phenotypes in L4 worms are due to defects in synapse elimination. Taken together, our results demonstrate that the activation of the CED pathway plays an important role in synapse elimination in vivo.

Axonal Mitochondria Are Required for Synapse Elimination

In cultured hippocampal neurons, dysfunction of mitochondria can promote synapse elimination through activation of caspase-3 (Ertürk et al., 2014). By examining a transgene marker expressing mitochondrial cytochrome c oxidase subunit 8 (Cox-8) Crimson fusion protein, we found that mitochondria are either

neurons in loss-of-function *ric-7* (resistance to inhibitors of cholinesterase), which is essential for axonal localization of mitochondria in *C. elegans* (Rawson et al., 2014). We observed that loss of function in *ric-7* blocked the distribution of mitochondria in D/V neurites and displayed elimination phenotypes to a similar degree as CED mutants (Figures 3A–3D). Moreover, double mutants of *ric-7* and CED genes did not enhance the elimination phenotypes, and loss of function in *ced-9* could suppress *ric-7(lf)* back to control level (Figures 3D and S2D), suggesting that axonal mitochondria can activate the CED pathway to regulate the elimination of synaptic components in RME neurons.

To address how axonal mitochondria affect the CED pathway, we generated transgene reporters labeling CED-3 in motor neurons and EGL-1 in RME neurons, and we found that CED-3 and EGL-1 were enriched at synaptic regions and co-localized with mitochondria (Figures S3B, S3C, and S3F). Remarkably, loss of function in *ric-7* completely blocked axonal/synaptic localization of CED-3 and CED-9 (Figures S3D and S3E), indicating that the axonal/synaptic localization of CED-9 and CED-3 depends on the presence of mitochondria in axons. Previous studies showed that transport of mitochondria in axons is mediated by a motor protein *unc-116* in motor neurons (Rawson et al., 2014). However, we did not observe any strong defects in mitochondrion distribution in RME neurons of *unc-116(lf)* animals, and overexpression of the mitochondrion-targeted kinesin (Kinesin-TOM7) did not rescue mitochondrion distribution or SNB-GFP elimination phenotypes in RME neurons of *ric-7(lf)* animals, suggesting that mitochondria may use distinct motor proteins in different neurons (Figures S3G–S3I). We next wanted to address whether the distribution of mitochondria in D/V neurites required the CED pathway. We found that disruption of the CED pathway did not affect mitochondria distribution, and loss of function in *ced-9* did not restore D/V mitochondria in *ric-7(lf)* animals (Figures S4A–S4E). Similar to the loss of function in the CED

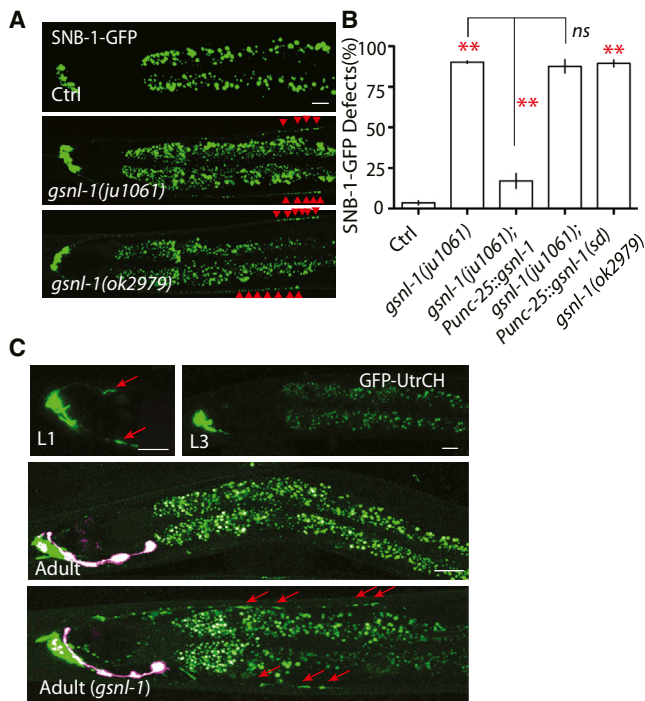


Figure 4. *gsnl-1* Regulates Actin Dynamics in Synapse Elimination (A and B) The F-actin-severing function of GSNL-1 is required for synapse elimination. (A) Images show two loss-of-function alleles of *gsnl-1* both prevent the elimination of synapses in RME neurons. Red arrowheads highlight D/V synapses. (B) *gsnl-1* acts cell autonomously to regulate synapse elimination, and deletion of the linker region required for its severing function abolishes *gsnl-1* functions in synapse elimination. (C) Loss of function in *gsnl-1* induces mis-accumulation of actin filaments in D/V neurites. Polymerized F-actin is visualized by GFP-utrCH. F-actin accumulates in D/V neurites at the similar position of D/V synapses at L1 stage, and becomes undetectable in those D/V neurites in L3 and adult animals. In adult *gsnl-1(lf)* mutants, the strong F-actin signal can still be observed in D/V neurites (red arrows). The pink neurons are AIY neurons from the expression of co-injection marker *Pttx-3-RFP*. In (B), experiments were performed at least three times, with $n \geq 80$ animals each time. For transgenic animals, the results shown here are generated from at least three independent lines. Data are shown as mean \pm SD. Student's t test, ** $p < 0.01$; ns, no significant difference. Scale bar, 10 μ m. See also Figures S4 and S5.

pathway, mutating *ric-7* also prevented SNB-1-GFP elimination in DD motor neurons (Figures S5A and S5B). In conclusion, our results show that axonal mitochondria act upstream of the CED pathway in the elimination of presynaptic components.

C. *elegans* Gelsolin Protein GSNL-1 Is Required for Synapse Elimination

Caspases are cysteine-aspartate proteases. Almost 1,000 proteins have been predicted to be cleaved by caspases (Crawford and Wells, 2011). What is the downstream target of the caspase CED-3 in synapse elimination? To answer this question, we analyzed other mutants isolated in our genetic screen that resembled *ced-3(lf)*-like phenotypes. One mutant, *ju1061*, caught our attention because it had strong SNB-1-GFP elimination defects, but, unlike CED mutants, had no additional

neurons, which suggests *ju1061* affects a non-apoptotic gene required for the elimination of presynaptic components. We mapped *ju1061* to the center region of chromosome V, and analysis of whole genomic sequencing results showed that only a single gene, *gsnl-1*, was altered in the region of interest. *gsnl-1* encodes a gelsolin-related protein that contains four conserved gelsolin domains (Klaavuniemi et al., 2008). *ju1061* induces a nonsense mutation in the third gelsolin domain (Figure S5C; Table S1). We found about 90% of *ju1061* adult animals showed SNB-1-GFP elimination defects, and expression of the *gsnl-1* genomic fragment in RME neurons rescued *ju1061* phenotypes (Figures 4A and 4B). A loss-of-function allele of *gsnl-1*, *ok2979*, displayed SNB-1-GFP and SYD-2-GFP elimination phenotypes similar to those in *ju1061* (Figures 4A, 4B, S6A, and S6B). Loss of function in *gsnl-1* also could suppress synapse elimination in DD motor neurons (Figures S7A and S7B). Previous studies showed that GSNL-1 can sever actin filaments in vitro, and a conserved linker region between the first and second gelsolin domains is required for its F-actin-severing function (Klaavuniemi et al., 2008; Liu et al., 2010). We found that expression of GSNL-1 lacking this linker region in RME neurons failed to rescue *ju1061* defects (Figure 4B). These results led us to conclude that *ju1061* is a loss-of-function allele of *gsnl-1*, and that the function of *gsnl-1* in SNB-1-GFP elimination relies on its F-actin-severing activity.

To further test if *gsnl-1* can regulate F-actin de-polymerization in RME D/V neurites, we made a reporter strain expressing GFP-UtrCH to label F-actin. UtrCH is the calponin homology domain of F-actin binding protein utrophin, and it has been shown to specifically bind F-actin in *C. elegans* (Chia et al., 2012). As shown in Figure 4C, F-actin was enriched at the end of RME D/V neurites where the transient synapses were formed in L1 animals, but no F-actin patch was observed in D/V neurites in L3 or later-stage animals (Figure 4C). This result is consistent with previous studies showing that the accumulation of F-actin is required for the formation of synapses (Chia et al., 2012). To test the function of *gsnl-1* in the regulation of F-actin in RME D/V neurites, we examined this marker in *gsnl-1* loss-of-function background and found strong accumulation of F-actin at the end of D/V neurites in adult animals (Figure 4C). In the DD motor neurons, we found that GFP-UtrCH was not only accumulated in axons, but also had strong signals in dendrites. As shown in Figure S6D, in L1 animals, DD neurons formed synapses at ventral cords, and dorsal processes functioned as dendrites, but GFP-UtrCH was accumulated in both ventral and dorsal cords. In L4 animals, DD neurons reversed their polarity to form synapses with dorsal muscles, and ventral processes served as dendrites to receive signals from other neurons. GFP-UtrCH had similar fluorescence intensity in dorsal and ventral cords in L4 animals (Figures S6D and S6F). We found that loss of function in *gsnl-1* induced accumulation of enlarged GFP-UtrCH patches at uneliminated transient synapses in ventral cords of L4 animals, and, as a result, the relative fluorescence intensity in ventral cords increased 50% (Figures S6E and S6F). These results suggest that de-polymerization of actin filaments in D/V neurites by *gsnl-1* is important for the elimination of transient synapses. Since loss of function in *gsnl-1* had similar phenotypes

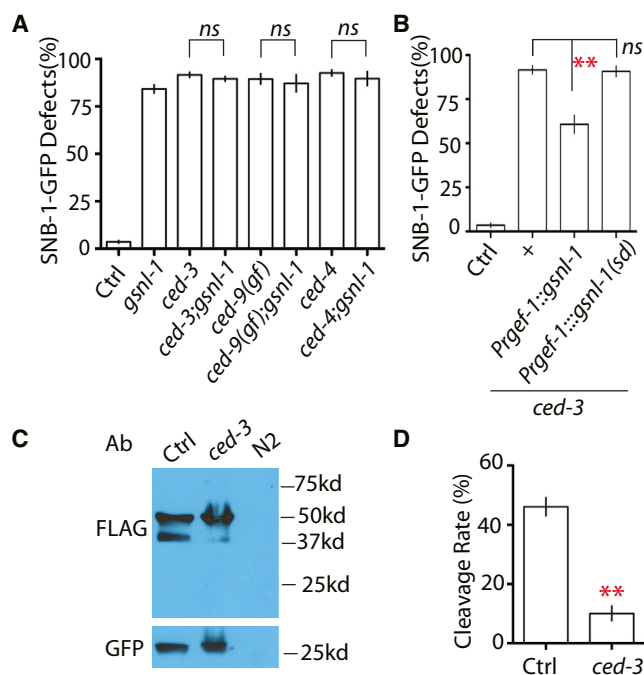


Figure 5. GSNL-1 Acts Downstream of CED-3 and Can Be Cleaved by CED-3

(A) *gsnl-1* acts in the same pathway with CED genes. Double mutants of *gsnl-1* and CED genes have a similar degree of SNB-1-GFP elimination defects as single mutants.

(B) The F-actin-severing function of *gsnl-1* is required for synapse elimination induced by activation of the CED pathway. Overexpression of *gsnl-1* can partially suppress *ced-3* phenotypes in RME neurons, and deleting the linker region required for the severing function abolishes its suppression ability on *ced-3(lf)*.

(C and D) CED-3 can cleave GSNL-1. (C) Western blotting analysis shows loss of function in *ced-3* suppresses the cleavage of GSNL-1. FLAG antibodies recognize the full-length (50 kDa) and the cleaved (40 kDa) GSNL-1. No signal was detected in wild-type N2 worms without the transgene. *Pttx-3::gfp* was used as a co-injection marker for *gsnl-1* transgene, and GFP was served as a loading control in western blot. (D) Quantification of cleavage rate of GSNL-1. Five independent experiments were performed, and band intensity was measured using ImageJ. The cleavage rate was calculated as follows: $P40 \text{ intensity} / (P50 \text{ intensity} + P40 \text{ intensity}) \times 100\%$.

In (A) and (B), experiments were performed at least three times, with $n \geq 80$ animals each time. For transgenic animals, the results shown here are generated from at least three independent lines. Data are shown as mean \pm SD. Student's t test, ** $p < 0.01$; ns, no significant difference.

as *ced-3(lf)*, we next wanted to test whether the CED pathway could promote the elimination of presynaptic components by activating GSNL-1.

GSNL-1 Is Cleaved by CED-3

One way to address the genetic interactions between *gsnl-1* and the CED pathway is to examine the double mutant phenotypes. If *ced;gsnl-1* double mutants show stronger phenotypes than each single mutant, we can conclude that *gsnl-1* and the CED pathway act in parallel during synapse elimination. If the double mutants do not enhance the single-mutant phenotypes, they likely function in the same signaling pathway. As shown in Fig-

ure 5A, double mutants of *gsnl-1* with *ced-3(lf)*, *ced-9(gf)*, and *ced-4(lf)* exhibited the same percentage of animals with defects as single-mutant animals. Moreover, we counted the number of SNB-1-GFP puncta in RME/V neurites of animals with elimination defects, and found double mutants of *ced-3;gsnl-1* did not change the number of SNB-1-GFP puncta (Figure S6G). Due to the close genetic positions between *gsnl-1* and *egl-1*, we were unable to analyze *gsnl-1 egl-1* double-mutant phenotypes. Nonetheless, our results support a conclusion that *gsnl-1* acts in the CED pathway to regulate elimination of presynaptic components. De-polymerization of F-actin by GSNL-1 could act either upstream of EGL-1 or downstream of CED-3.

In vitro studies showed the F-actin-severing ability of GSNL-1 correlated with its protein level (Klaavuniemi et al., 2008). To test where GSNL-1 is in the CED pathway, we overexpressed *gsnl-1* in the nervous system, and found increasing *gsnl-1* expression levels partially suppressed *ced-3(lf)* phenotypes (Figure 5B). More importantly, the function of *gsnl-1* in the CED pathway relied on its F-actin-severing activity, because deleting the linker region required for F-actin-severing function from GSNL-1 totally abolished its suppression ability (Figure 5B). Combining these results, we concluded that GSNL-1 acts downstream of CED-3 and that its activation is positively regulated by CED-3. One major mechanism by which caspases regulate downstream targets is to cleave proteins at cysteine-aspartate sites. To test whether CED-3 can cleave GSNL-1, we generated a reporter expressing N-terminal FLAG-tagged GSNL-1 (*yad1s10*) in the nervous system. In wild-type background, we detected two protein products around 50 and 40 kDa (Figure 5C). Since the predicted molecular weight for full-length GSNL-1 is 52 kDa, the 40-kDa band is a product of cleavage of GSNL-1. Remarkably, loss of function in *ced-3* strongly blocked the production of the 40-kDa band such that only about 10% GSNL-1 proteins were cleaved in *ced-3(lf)*, compared to 45% in control animals (Figures 5C and 5D). Now knowing GSNL-1 acts downstream of and can be cleaved by CED-3, what is the significance of this cleavage in synapse elimination?

The CED Pathway Promotes F-actin Disassembly through Cleavage of GSNL-1 at a Conserved C-terminal Region

GSNL-1 can be cleaved by CED-3 to a fragment around 40 kDa at the C terminus, indicating the cleavage site is between amino acids 350 and 400. Using online caspase substrate prediction server CASVM (<http://www.casbase.org/casvm/index.html>), we found one conserved potential caspase site in the region of interest (Figure 6A). To test whether CED-3 can cleave GSNL-1 at this site, we generated transgenes expressing mutated GSNL-1 proteins without this cut site or changing the critical aspartate to alanine, and we found that both mutations completely blocked the cleavage of GSNL-1 (Figure 6B). Next, we asked whether the cleavage by CED-3 is required for the *gsnl-1* function. We compared the rescue ability of wild-type and the CED-3 cleavage-site-deleted *gsnl-1*. The results showed that, compared to wild-type *gsnl-1*, deletion of the CED-3 cleavage site strongly reduced the rescuing ability of *gsnl-1*, indicating the importance of CED-3 cleavage in regulation of *gsnl-1* activation (Figure 6C). The partial rescue of *gsnl-1(lf)* by the CED-3

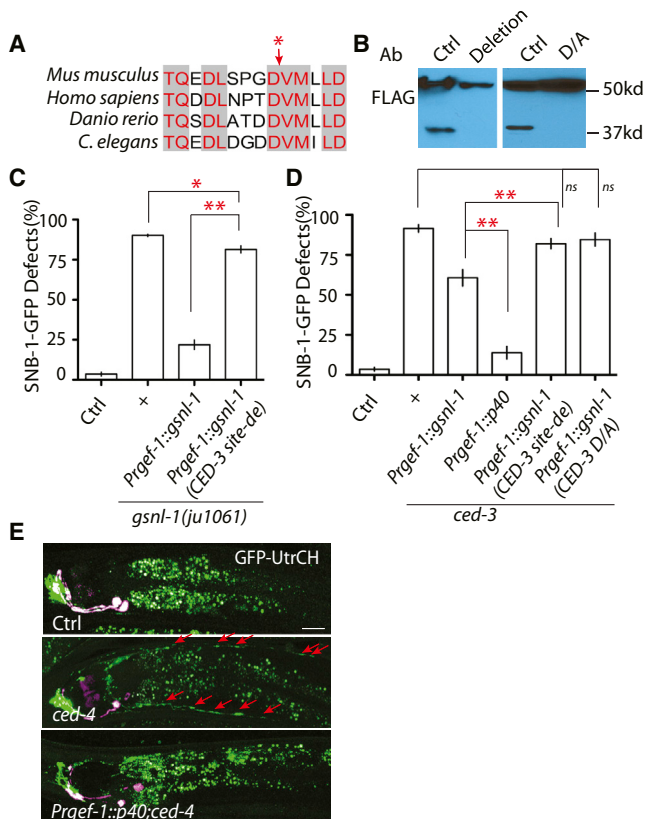


Figure 6. CED-3 Cleaves GSNL-1 at a C-terminal Conserved Site to Promote Its F-actin-Severing Ability

(A) Sequence analysis identifies a conserved candidate caspase cleavage site at the region where cleavage can produce a 40-kb band in *C. elegans*. NCBI Reference Sequence: *Danio rerio* XP_003198825.1; *Mus musculus* (gene: Advillin) XP_006513165.1; *Homo sapiens* (Gene: Advillin) NP_006567.3. The red asterisk points to the potential cut site.

(B) Deletion of the five core amino acids DDVMI (deletion) or mutating the aspartate (DDVMI) to alanine (DAVMI) (D/A) in this region blocks the cleavage of GSNL-1.

(C) Deletion of the CED cleavage site strongly affects *gsnl-1* functions. Expression of *gsnl-1* lacking the CED cleavage site only shows weak rescue ability, while wild-type *gsnl-1* rescues mutant phenotypes in over 90% of animals.

(D) Expression of the cleaved GSNL-1 can bypass the requirement of *ced-3* in synapse elimination. Expression of P40 almost totally suppresses *ced-3* phenotypes, while un-cleavable GSNL-1 fails to suppress *ced-3* phenotypes. (E) Loss of function in the CED pathway induces mis-accumulation of F-actin in D/V neurites, and overexpression of P40 can suppress the effect of *ced-4(lf)*. In (C) and (D), experiments were performed at least three times, with $n \geq 80$ animals each time. For transgenic animals, the results shown here are generated from at least three independent lines. Data are shown as mean \pm SD. Student's t test, ** $p < 0.01$, * $p < 0.05$; ns, no significant difference.

cleavage-site-deleted *gsnl-1* suggests other mechanisms may regulate *gsnl-1* activation (Figure 6C).

To further confirm the cleaved GSNL-1 is the active form, we expressed P40, a truncated GSNL-1 protein representing the cleavage product by CED-3, in *ced-3(lf)* animals. As shown in Figure 6D, overexpression of P40 suppressed *ced-3(lf)* much better than that of full-length GSNL-1. Consistent with this

observation, deletion of the CED-3 site or mutating the critical aspartate to alanine in GSNL-1 totally abolished its suppression ability on *ced-3(lf)* phenotypes (Figure 6D). Previous in vitro studies (Klaavuniemi et al., 2008) and our results here show one major function of GSNL-1 is to sever actin filaments. To test whether the CED pathway was involved in the regulation of F-actin, we compared F-actin distribution in control and mutant animals. We found that *ced-4(lf)*, *egl-1(lf)*, *ric-7(lf)*, and *ced-9(gf)* induced mis-accumulation of F-actin in RMED/V neurites in all animals observed (≥ 100 animals for each genotype) (Figures 6E and S7C–S7E). Similar to what we observed in *gsnl-1(lf)* animals, F-actin formed enlarged patches in dorsal processes of DD neurons in L4 animals of mutants affecting each member of the CED pathway and *ric-7* (Figures S7F and S7G). Furthermore, the effect of CED mutants and *ric-7(lf)* could be completely suppressed by the expression of P40, the active form GSNL-1, in all animals observed (≥ 70 animals for each genotype) (Figures 6E and S7C–S7E). Taken together, our results demonstrate that the cleavage of GSNL-1 at the conserved C-terminal site by CED-3 promotes its activation and triggers F-actin de-polymerization to eliminate synaptic components during development.

DISCUSSION

Using the development of *C. elegans* RME neurons, we investigated the molecular mechanisms of synapse elimination. During development RME D/V neurons form transient clusters of presynaptic components in D/V neurites at L1 stage, and those clusters are eliminated before L3 stage. In EM studies, we uncovered RMED/V neurites contained swelling structures enriched with vesicles, but the nature of these swellings is unknown. Among many possibilities, one could be that they might represent immature synapses, as our analyses of presynaptic markers showed strong correlation with these swellings. In *C. elegans*, the DD motor neurons form synapses at the ventral cord at the L1 stage, and those synapses are eliminated in the L2 stage. Although the SNB-1-GFP puncta in RME D/V dendrites may not represent mature synapses, the consistent phenotypes of multiple fluorescent reporters from DD motor neurons and RME neurons supports that the apoptotic CED pathway can regulate some aspects of synapse elimination in vivo. Taking advantage of the powerful genetic tools in *C. elegans*, we further uncovered the important roles of axonal mitochondria and F-actin-severing protein GSNL-1 in the elimination of presynaptic materials. Finally, we demonstrated that the caspase CED-3 cleaves GSNL-1 at a conserved site to promote GSNL-1 activation. Therefore, our working model is that during development some internal cues trigger the local activation of the CED pathway through mitochondria to activate GSNL-1 by protein cleavage, and the activated GSNL-1 promotes disassembly of the F-actin network at synaptic regions to induce the elimination of synaptic components (Figure 7).

Cell Death and Synapse Elimination

It has long been known that the activation of apoptosis pathway triggers cell death (Hyman and Yuan, 2012). Previous studies (Ertürk et al., 2014; Wang et al., 2014) and our results here show that

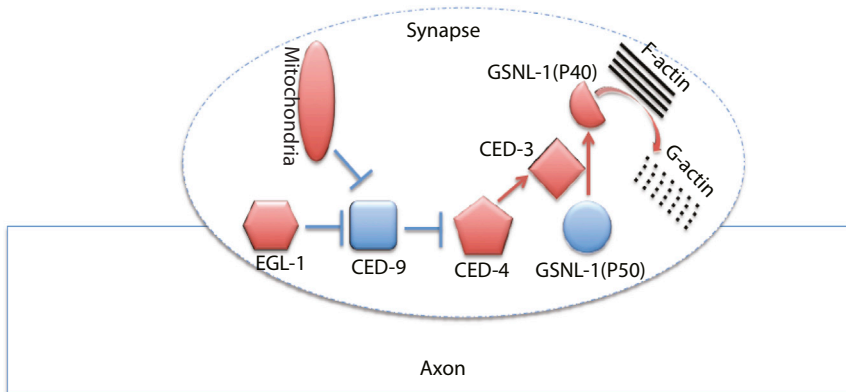


Figure 7. A Working Model for the Regulation of Mitochondria-CED-GSNL-1 in Synapse Elimination

Axonal mitochondria activate the CED pathway to promote the cleavage of GSNL-1, and then the cleaved GSNL-1(P40) disassembles the F-actin network to eliminate synapses.

activation of the apoptosis pathway can promote synapse elimination without loss of neurons during development. The question is how neurons restrict the activation of the caspase pathway only at synaptic regions to prevent cell death from happening. Actin is an ubiquitous component of all types of cells and is involved in almost all biological processes. It is not a surprise that, as a major F-actin-severing protein family, gelsolin proteins play important roles in the regulation of cell death. The first study that linked gelsolin with apoptosis was in cultured Jurkat cells, in which overexpression of gelsolin inhibited the activation of CPP32 protease (caspase-3) to prevent cell death induced by treatment of anti-FAS antibodies (Ohtsu et al., 1997). Since then gelsolin has been shown to inhibit apoptosis through directly binding with caspase-9 and caspase-3, preventing mitochondrial membrane potential loss and cytochrome c release, blocking mitochondrial voltage-dependent anion channel, and de-polymerization of F-actin (Azuma et al., 2000; Harms et al., 2004; Koya et al., 2000; Kusano et al., 2000). Activation of gelsolin also has been reported to play anti-apoptosis roles in human epidermoid cancer cells, oncogenic K-ras mutation cell lines, thermal injury, and neural loss (Boccellino et al., 2004; Harms et al., 2004; Klampfer et al., 2004; Zhang et al., 2011). However, an increase in gelsolin activity failed to prevent apoptosis in lymphocyte and fas antibody-induced liver failure in vivo (Leifeld et al., 2006; Posey et al., 2000). Nevertheless, gelsolin proteins can play anti-apoptotic roles in caspase-mediated cell death. In our studies, we found that activation of the apoptosis pathway promotes GSNL-1 activation through cleavage at the C-terminal conserved site. It is possible that the activated GSNL-1 generated by local activation of the CED pathway can inhibit further activation of caspases, thereby restricting activation of the apoptosis pathway only at certain subcellular regions to prevent cell death from happening.

Calcium, Caspases, Gelsolin, and Synapse Elimination

In the mammalian cortex, synaptic elimination starts from the late postnatal period until the end of life. In multiple regions of cortex, studies have showed blockage of NMDA receptors prevents the loss of synapses in vivo (Ohno et al., 2010; Rabacchi et al., 1992). In LTD, the shrinkage of dendritic spines relies on the activation of NMDA receptors (Zhou et al., 2004). In neurodegenerative diseases, synapse loss happens in an

NMDA-receptor-dependent manner (Milnerwood and Raymond, 2010). Calcium channels, such as voltage-dependent calcium channels and TRP channels, also were found to be important for synapse elimination (Gibson et al., 2008; Hashimoto et al., 2011). These studies support the essential role of calcium in the regulation of synapse elimination. In the *C. elegans* CED pathway, CED-4 is an Apaf-1-like protein and contains two EF-hand calcium-binding domains (Yuan and Horvitz, 1992). In axon regeneration, elevation of calcium concentration upon injury can activate CED-4 to promote axonal regrowth (Pinan-Lucarre et al., 2012). The second gelsolin domain of GSNL-1 can change its conformation upon binding with calcium to regulate its F-actin-severing ability (Liu et al., 2011). These findings suggest that change in local calcium concentration, either by neuronal activity or ER/mitochondrial release, may modulate the strength of the CED-GSNL-1 pathway in synapse elimination.

Caspases and Gelsolin

Gelsolin was one of the first caspase substrates identified using in vitro assays (Kothakota et al., 1997). The fragmentation of gelsolin by caspases contributes to the morphological change of apoptotic cells (Kothakota et al., 1997). Neuronal cleavage of gelsolin is reported in Alzheimer's disease, spinal cord injury, ischemia, and burn injury (Ji et al., 2009; Matsushita et al., 2000; Springer et al., 1999; Zhang et al., 2013). However, these studies have focused mainly on the apoptotic roles of caspase-mediated gelsolin cleavage in the nervous system. During aging and in disease conditions, neurodegeneration often happens in a dying-back manner that starts from abnormal pruning of pre-synaptic and post-synaptic structures, and then the degeneration progresses along axons and dendrites, and finally the dying signal induces the loss of neurons (Adalbert and Coleman, 2012; Wang et al., 2012). Several studies have showed that prevention of the early degeneration events at synapses and axons can protect neurons from death (Ferri et al., 2003; George and Griffin, 1994; Kaneko et al., 2006; Meyer zu Horste et al., 2011). Although our findings highlight the role of CED-GSNL-1 regulation in synapse elimination during development, the same mechanism also could be applied to synapse elimination in aging or disease conditions, and may provide a new angle for understanding the function of the CED pathway in those processes.

Synapse Elimination and Axon Regeneration

In our experiments, we expressed GSNL-1 in all neurons and detected cleavage of GSNL-1, suggesting the CED-GSNL-1 regulation also may function in other processes. Recent studies

in *C. elegans* revealed the important role of CED-4 and CED-3 in axon regeneration. Using mechanosensory ALM neurons as a model, Pinan-Lucarre and colleagues showed that axons sprout out filopodia-like processes shortly after injury, and loss of function in both *ced-4* and *ced-3* blocks the formation of those filopodia structures and eventually suppresses regeneration (Pinan-Lucarre et al., 2012). The filopodia structure in regenerating axons is similar to that in growth cones during axon path-finding. Extensive studies showed that actin dynamics are the major cause for filopodia growth and retraction in axon guidance (Luo, 2002). More interestingly, the caspase-mediated gelsolin cleavage was observed after spinal cord injury (Springer et al., 1999). Therefore, it is possible that, in axon regeneration, CED-3 also may cleave GSNL-1 to regulate F-actin assembly and filopodia formation after injury. One key regulator for axon regeneration in *C. elegans* is DLK-1 (Hammarlund and Jin, 2014). Genetic studies showed CED-3 acts in the same pathway with DLK-1 in regeneration (Pinan-Lucarre et al., 2012). DLK-1 is required both for the re-initiation of growth cones and elongation of axons. Regulation of microtubule dynamics by the DLK-1 pathway has been shown to be important for the elongation of regenerating axons (Ghosh-Roy et al., 2012). But promoting microtubule assembly can only partially rescue *dlk-1* phenotypes, suggesting additional components are required in the early period of regeneration (Ghosh-Roy et al., 2012). It will be interesting to test whether the CED-3-mediated actin regulation is controlled by DLK-1 during the rebuilding of growth cones after injury.

EXPERIMENTAL PROCEDURES

C. elegans Genetics

We maintained *C. elegans* strains on NGM plates at 20°C–22.5°C as described previously (Brenner, 1974). All transgenes and strains are described in Tables S1 and S2. We used *juls1* (*Punc-25::SNB-1-GFP*) (Hallam and Jin, 1998) in *unc-30* (*ju32*) background (Table S1) to visualize RME neuron presynaptic terminals, and we used *juls137* (*Pflp-13::SNB-1-GFP*) (Abrams et al., 2008) to visualize DD motor neuron synapses. *hpls3* (*Punc-25::SYD-2-GFP*) (Yeh et al., 2009) was used to visualize RME presynaptic active zones. *unc-30* (*ju32*) was isolated by Mei Zhen and Y.J. in an early screen for synapse formation defects and contained a G to A mutation in the 3' splice acceptor of the last intron. *ced-3* (*ju1056*) and *gsnl-1* (*ju1061*) were isolated from the strain CZ15720 *unc-30* (*ju32*) *juls1* (*Punc-25::SNB-1-GFP*) after ethyl methanesulfonate mutagenesis.

Fluorescence Microscopy

We scored fluorescent reporters in live animals using a Zeiss Axio Imager 2 microscope equipped with Chroma HQ filters. For quantification of RME neuron synapse elimination defects, at least three independent experiments were performed and a total of 200–400 1-day-old adults were analyzed. DD motor neuron phenotypes were analyzed at the L1, L4, and 2-day-adult stages. Confocal images were collected at animals immobilized in 1% 1-phenoxy-2-propanol (TCI America) in M9 buffer using a Zeiss LSM700 confocal microscope. Pictures shown in the figures are z stack images (1 μm/section).

Statistical Analysis

We analyzed our data using one-tailed Student's t test in GraphPad Prism.

Protein Analysis

For expression studies in *C. elegans*, we used an integrated transgene (*yadIs10*) expressing FLAG-GSNL-1 driven by a pan-neuronal promoter *Prgef-1* (PNYL99). Synchronous animals were collected at L2 stages, and

protein lysis in SDS sample buffer containing 1 mM DTT were obtained by freeze-thaw 20–50 times in dry ice/ethanol and 37°C water bath, then denatured by heating to 95°C for 5 min. Blots were probed with rabbit anti-Flag antibodies (Sigma, F1804) or a mouse anti-GFP monoclonal antibody (Sigma, G1544), and they were visualized with HRP-conjugated anti-rabbit or anti-mouse secondary antibodies at 1:5,000 (Amersham) using the SuperSignal West Femto kit (Pierce).

DNA Constructs and Generation of Transgenes

All DNA expression constructs were made using Gateway cloning technology (Invitrogen). Sequences of the final clones were confirmed. The information for each construct is in Table S2. The primer sequences are available upon request.

Transgenic animals were generated following standard procedures (Mello et al., 1991). In general, plasmid DNAs of interest were used at 1–50 ng/μl with the co-injection marker *Pttx-3-RFP* or *Pttx-3-GFP* at 50 ng/μl. For each construct, three to ten independent transgenic lines were analyzed. Table S2 lists the genotypes and DNA constructs for the transgenes.

Electron Microscopy

L1 worms were fixed by high-pressure freezing followed by freeze substitution as previously described (Hung et al., 2013; Rostaing et al., 2004; Stigloher et al., 2011). The worm was cut into 70-nm-thick serial sections. Images were taken on an FEI Tecnai 20 electron microscope with an AMT 16000 digital camera, at 1.4 nm/pixel for reconstruction of the posterior processes and 0.3 nm/pixel for the images shown of the neurite swellings. Images were stitched and aligned using TrakEM2 (Cardona et al., 2012). RMED and RMEV were identified based on their cell body position (Sulston, 1983) and the trajectory of their neurites (White et al., 1986), and they were reconstructed volumetrically within TrakEM2.

SUPPLEMENTAL INFORMATION

Supplemental Information includes seven figures and two tables and can be found with this article online at <http://dx.doi.org/10.1016/j.celrep.2015.05.031>.

AUTHOR CONTRIBUTIONS

D.Y. and L.M. designed and performed the experiments. B.M., S.J.C., and M.N. carried out the EM analysis. B.M. analyzed the EM data. A.W. did all western blot analysis. Y.J. provided some strains in this study. The genetic screen for RME development was carried out by D.Y. when he was a postdoctoral fellow in Y.J.'s lab. L.M. and D.Y. wrote the manuscript.

ACKNOWLEDGMENTS

We thank Drs. Mei Zhen, Aravi Samuel, and Jeff Lichtman for the EM analysis. Some strains used in this study were provided by the Caenorhabditis Genetics Center (CGC), which is funded by NIH Office of Research Infrastructure Programs (P40 OD010440). We thank Dr. Yuji Kohara for cDNAs, Dr. Erik Jorgensen for Kinesin-TOM7 plasmid, Dr. Joachim Kurth for Apoliner reporter, and Dr. Mei Zhen for the active zone reporter and contribution in the isolation of *unc-30* (*ju32*). We thank our lab members for comments on the manuscript. The *C. elegans* L1 EM project is supported by the Human Frontier Science Program (HFSP RGP0051/2014 to Aravi Samuel, Jeff Lichtman, and Mei Zhen). S.J.C. is supported by NIH Grant 5T32GM007491 awarded to the Albert Einstein College of Medicine. B.M. is supported by CIHR grants MOP 123250 and MOP 74530. Y.J. is an Investigator of the Howard Hughes Medical Institute. Part of the work was supported by grants from NIH (R01 NS035546 to Y.J. and K99NS076646 to D.Y.). The D.Y. lab is supported by R00 award (NS076646) from the National Institute of Neurological Disorders and Stroke.

Received: September 9, 2014

Revised: May 1, 2015

Accepted: May 15, 2015

Published: June 11, 2015

REFERENCES

- Abrams, B., Grill, B., Huang, X., and Jin, Y. (2008). Cellular and molecular determinants targeting the *Caenorhabditis elegans* PHR protein RPM-1 to perisynaptic regions. *Dev. Dyn.* 237, 630–639.
- Adalbert, R., and Coleman, M.P. (2012). Axon pathology in age-related neurodegenerative disorders. *Neuropathol. Appl. Neurobiol.*
- Azuma, T., Kohts, K., Flanagan, L., and Kwiatkowski, D. (2000). Gelsolin in complex with phosphatidylinositol 4,5-bisphosphate inhibits caspase-3 and -9 to retard apoptotic progression. *J. Biol. Chem.* 275, 3761–3766.
- Boccellino, M., Giuberti, G., Quagliuolo, L., Marra, M., D'Alessandro, A.M., Fujita, H., Giovane, A., Abbruzzese, A., and Caraglia, M. (2004). Apoptosis induced by interferon-alpha and antagonized by EGF is regulated by caspase-3-mediated cleavage of gelsolin in human epidermoid cancer cells. *J. Cell. Physiol.* 201, 71–83.
- Brenner, S. (1974). The genetics of *Caenorhabditis elegans*. *Genetics* 77, 71–94.
- Campbell, D.S., and Holt, C.E. (2003). Apoptotic pathway and MAPKs differentially regulate chemotropic responses of retinal growth cones. *Neuron* 37, 939–952.
- Cardona, A., Saalfeld, S., Schindelin, J., Arganda-Carreras, I., Preibisch, S., Longair, M., Tomancak, P., Hartenstein, V., and Douglas, R.J. (2012). TrakEM2 software for neural circuit reconstruction. *PLoS One* 7, e38011.
- Chia, P.H., Patel, M.R., and Shen, K. (2012). NAB-1 instructs synapse assembly by linking adhesion molecules and F-actin to active zone proteins. *Nat. Neurosci.* 15, 234–242.
- Chia, P.H., Chen, B., Li, P., Rosen, M.K., and Shen, K. (2014). Local F-actin network links synapse formation and axon branching. *Cell* 156, 208–220.
- Crawford, E.D., and Wells, J.A. (2011). Caspase substrates and cellular remodeling. *Annu. Rev. Biochem.* 80, 1055–1087.
- Doussau, F., and Augustine, G.J. (2000). The actin cytoskeleton and neurotransmitter release: an overview. *Biochimie* 82, 353–363.
- Ertürk, A., Wang, Y., and Sheng, M. (2014). Local pruning of dendrites and spines by caspase-3-dependent and proteasome-limited mechanisms. *J. Neurosci.* 34, 1672–1688.
- Ferri, A., Sanes, J.R., Coleman, M.P., Cunningham, J.M., and Kato, A.C. (2003). Inhibiting axon degeneration and synapse loss attenuates apoptosis and disease progression in a mouse model of motoneuron disease. *Curr. Biol.* 13, 669–673.
- Flavell, S.W., and Greenberg, M.E. (2008). Signaling mechanisms linking neuronal activity to gene expression and plasticity of the nervous system. *Annu. Rev. Neurosci.* 31, 563–590.
- George, R., and Griffin, J.W. (1994). Delayed macrophage responses and myelin clearance during Wallerian degeneration in the central nervous system: the dorsal radiculotomy model. *Exp. Neurol.* 129, 225–236.
- Ghosh-Roy, A., Goncharov, A., Jin, Y., and Chisholm, A.D. (2012). Kinesin-13 and tubulin posttranslational modifications regulate microtubule growth in axon regeneration. *Dev. Cell* 23, 716–728.
- Gibson, H.E., Edwards, J.G., Page, R.S., Van Hook, M.J., and Kauer, J.A. (2008). TRPV1 channels mediate long-term depression at synapses on hippocampal interneurons. *Neuron* 57, 746–759.
- Hall, D.H., and Hedgecock, E.M. (1991). Kinesin-related gene *unc-104* is required for axonal transport of synaptic vesicles in *C. elegans*. *Cell* 65, 837–847.
- Hallam, S.J., and Jin, Y. (1998). *lin-14* regulates the timing of synaptic remodeling in *Caenorhabditis elegans*. *Nature* 395, 78–82.
- Hammarlund, M., and Jin, Y. (2014). Axon regeneration in *C. elegans*. *Curr. Opin. Neurobiol.* 27, 199–207.
- Harms, C., Bösel, J., Lautenschlager, M., Harms, U., Braun, J.S., Hörtnagl, H., Dirnagl, U., Kwiatkowski, D.J., Fink, K., and Endres, M. (2004). Neuronal gelsolin prevents apoptosis by enhancing actin depolymerization. *Mol. Cell. Neurosci.* 25, 69–82.
- Hashimoto, K., Tsujita, M., Miyazaki, T., Kitamura, K., Yamazaki, M., Shin, H.S., Watanabe, M., Sakimura, K., and Kano, M. (2011). Postsynaptic P/Q-type Ca²⁺ channel in Purkinje cell mediates synaptic competition and elimination in developing cerebellum. *Proc. Natl. Acad. Sci. USA* 108, 9987–9992.
- Huesmann, G.R., and Clayton, D.F. (2006). Dynamic role of postsynaptic caspase-3 and BIRC4 in zebra finch song-response habituation. *Neuron* 52, 1061–1072.
- Hung, W.L., Hwang, C., Gao, S., Liao, E.H., Chitturi, J., Wang, Y., Li, H., Stigloher, C., Bessereau, J.L., and Zhen, M. (2013). Attenuation of insulin signaling contributes to FSN-1-mediated regulation of synapse development. *EMBO J.* 32, 1745–1760.
- Huttenlocher, P.R., de Courten, C., Garey, L.J., and Van der Loos, H. (1982). Synaptogenesis in human visual cortex—evidence for synapse elimination during normal development. *Neurosci. Lett.* 33, 247–252.
- Hyman, B.T., and Yuan, J. (2012). Apoptotic and non-apoptotic roles of caspases in neuronal physiology and pathophysiology. *Nat. Rev. Neurosci.* 13, 395–406.
- Ji, L., Chauhan, A., Wegiel, J., Essa, M.M., and Chauhan, V. (2009). Gelsolin is proteolytically cleaved in the brains of individuals with Alzheimer's disease. *J. Alzheimers Dis.* 18, 105–111.
- Jiao, S., and Li, Z. (2011). Nonapoptotic function of BAD and BAX in long-term depression of synaptic transmission. *Neuron* 70, 758–772.
- Kakizawa, S., Yamasaki, M., Watanabe, M., and Kano, M. (2000). Critical period for activity-dependent synapse elimination in developing cerebellum. *J. Neurosci.* 20, 4954–4961.
- Kamiyama, T., Yoshioka, N., and Sakurai, M. (2006). Synapse elimination in the corticospinal projection during the early postnatal period. *J. Neurophysiol.* 95, 2304–2313.
- Kaneko, S., Wang, J., Kaneko, M., Yiu, G., Hurrell, J.M., Chitnis, T., Khoury, S.J., and He, Z. (2006). Protecting axonal degeneration by increasing nicotinamide adenine dinucleotide levels in experimental autoimmune encephalomyelitis models. *J. Neurosci.* 26, 9794–9804.
- Keller-Peck, C.R., Walsh, M.K., Gan, W.B., Feng, G., Sanes, J.R., and Lichtman, J.W. (2001). Asynchronous synapse elimination in neonatal motor units: studies using GFP transgenic mice. *Neuron* 31, 381–394.
- Klaavuniemi, T., Yamashiro, S., and Ono, S. (2008). *Caenorhabditis elegans* gelsolin-like protein 1 is a novel actin filament-severing protein with four gelsolin-like repeats. *J. Biol. Chem.* 283, 26071–26080.
- Klampfer, L., Huang, J., Sasazuki, T., Shirasawa, S., and Augenlicht, L. (2004). Oncogenic Ras promotes butyrate-induced apoptosis through inhibition of gelsolin expression. *J. Biol. Chem.* 279, 36680–36688.
- Kothakota, S., Azuma, T., Reinhard, C., Klippel, A., Tang, J., Chu, K., McGarry, T.J., Kirschner, M.W., Kohts, K., Kwiatkowski, D.J., and Williams, L.T. (1997). Caspase-3-generated fragment of gelsolin: effector of morphological change in apoptosis. *Science* 278, 294–298.
- Koya, R.C., Fujita, H., Shimizu, S., Ohtsu, M., Takimoto, M., Tsujimoto, Y., and Kuzumaki, N. (2000). Gelsolin inhibits apoptosis by blocking mitochondrial membrane potential loss and cytochrome c release. *J. Biol. Chem.* 275, 15343–15349.
- Kuo, C.T., Zhu, S., Younger, S., Jan, L.Y., and Jan, Y.N. (2006). Identification of E2/E3 ubiquitinating enzymes and caspase activity regulating *Drosophila* sensory neuron dendrite pruning. *Neuron* 51, 283–290.
- Kusano, H., Shimizu, S., Koya, R.C., Fujita, H., Kamada, S., Kuzumaki, N., and Tsujimoto, Y. (2000). Human gelsolin prevents apoptosis by inhibiting apoptotic mitochondrial changes via closing VDAC. *Oncogene* 19, 4807–4814.
- Leifeld, L., Fink, K., Debska, G., Fielenbach, M., Schmitz, V., Sauerbruch, T., and Spengler, U. (2006). Anti-apoptotic function of gelsolin in *fas* antibody-induced liver failure in vivo. *Am. J. Pathol.* 168, 778–785.
- Li, Z., Jo, J., Jia, J.M., Lo, S.C., Whitcomb, D.J., Jiao, S., Cho, K., and Sheng, M. (2010). Caspase-3 activation via mitochondria is required for long-term depression and AMPA receptor internalization. *Cell* 141, 859–871.
- Liu, Z., Klaavuniemi, T., and Ono, S. (2010). Distinct roles of four gelsolin-like domains of *Caenorhabditis elegans* gelsolin-like protein-1 in actin filament severing, barbed end capping, and phosphoinositide binding. *Biochemistry* 49, 4349–4360.

- Liu, Z., Kanzawa, N., and Ono, S. (2011). Calcium-sensitive activity and conformation of *Caenorhabditis elegans* gelsolin-like protein 1 are altered by mutations in the first gelsolin-like domain. *J. Biol. Chem.* *286*, 34051–34059.
- Luo, L. (2002). Actin cytoskeleton regulation in neuronal morphogenesis and structural plasticity. *Annu. Rev. Cell Dev. Biol.* *18*, 601–635.
- Luo, Z.G., Wang, Q., Zhou, J.Z., Wang, J., Luo, Z., Liu, M., He, X., Wynshaw-Boris, A., Xiong, W.C., Lu, B., and Mei, L. (2002). Regulation of AChR clustering by Dishevelled interacting with MuSK and PAK1. *Neuron* *35*, 489–505.
- Matsushita, K., Wu, Y., Qiu, J., Lang-Lazdunski, L., Hirt, L., Waeber, C., Hyman, B.T., Yuan, J., and Moskowitz, M.A. (2000). Fas receptor and neuronal cell death after spinal cord ischemia. *J. Neurosci.* *20*, 6879–6887.
- Mello, C.C., Kramer, J.M., Stinchcomb, D., and Ambros, V. (1991). Efficient gene transfer in *C.elegans*: extrachromosomal maintenance and integration of transforming sequences. *EMBO J.* *10*, 3959–3970.
- Meyer zu Horste, G., Miesbach, T.A., Muller, J.I., Fledrich, R., Stassart, R.M., Kieseier, B.C., Coleman, M.P., and Sereda, M.W. (2011). The Wlds transgene reduces axon loss in a Charcot-Marie-Tooth disease 1A rat model and nicotinamide delays post-traumatic axonal degeneration. *Neurobiol. Dis.* *42*, 1–8.
- Milnerwood, A.J., and Raymond, L.A. (2010). Early synaptic pathophysiology in neurodegeneration: insights from Huntington's disease. *Trends Neurosci.* *33*, 513–523.
- Murthy, V.N., and De Camilli, P. (2003). Cell biology of the presynaptic terminal. *Annu. Rev. Neurosci.* *26*, 701–728.
- Nelson, P.G., Fields, R.D., Yu, C., and Liu, Y. (1993). Synapse elimination from the mouse neuromuscular junction in vitro: a non-Hebbian activity-dependent process. *J. Neurobiol.* *24*, 1517–1530.
- O'Donnell, M., Chance, R.K., and Bashaw, G.J. (2009). Axon growth and guidance: receptor regulation and signal transduction. *Annu. Rev. Neurosci.* *32*, 383–412.
- Ohno, T., Maeda, H., Murabe, N., Kamiyama, T., Yoshioka, N., Mishina, M., and Sakurai, M. (2010). Specific involvement of postsynaptic GluN2B-containing NMDA receptors in the developmental elimination of corticospinal synapses. *Proc. Natl. Acad. Sci. USA* *107*, 15252–15257.
- Ohsawa, S., Hamada, S., Kuida, K., Yoshida, H., Igaki, T., and Miura, M. (2010). Maturation of the olfactory sensory neurons by Apaf-1/caspase-9-mediated caspase activity. *Proc. Natl. Acad. Sci. USA* *107*, 13366–13371.
- Ohtsu, M., Sakai, N., Fujita, H., Kashiwagi, M., Gasa, S., Shimizu, S., Eguchi, Y., Tsujimoto, Y., Sakiyama, Y., Kobayashi, K., and Kuzumaki, N. (1997). Inhibition of apoptosis by the actin-regulatory protein gelsolin. *EMBO J.* *16*, 4650–4656.
- Pinan-Lucarre, B., Gabel, C.V., Reina, C.P., Hulme, S.E., Shevkopylas, S.S., Slone, R.D., Xue, J., Qiao, Y., Weisberg, S., Roodhouse, K., et al. (2012). The core apoptotic executioner proteins CED-3 and CED-4 promote initiation of neuronal regeneration in *Caenorhabditis elegans*. *PLoS Biol.* *10*, e1001331.
- Posey, S.C., Martelli, M.P., Azuma, T., Kwiatkowski, D.J., and Bierer, B.E. (2000). Failure of gelsolin overexpression to regulate lymphocyte apoptosis. *Blood* *95*, 3483–3488.
- Rabacchi, S., Bailly, Y., Delhaye-Bouchaud, N., and Mariani, J. (1992). Involvement of the N-methyl-D-aspartate (NMDA) receptor in synapse elimination during cerebellar development. *Science* *256*, 1823–1825.
- Rawson, R.L., Yam, L., Weimer, R.M., Bend, E.G., Hartweg, E., Horvitz, H.R., Clark, S.G., and Jorgensen, E.M. (2014). Axons degenerate in the absence of mitochondria in *C. elegans*. *Curr. Biol.* *24*, 760–765.
- Rosenthal, J.L., and Taraskevich, P.S. (1977). Reduction of multiaxonal innervation at the neuromuscular junction of the rat during development. *J. Physiol.* *270*, 299–310.
- Rostaing, P., Weimer, R.M., Jorgensen, E.M., Triller, A., and Bessereau, J.L. (2004). Preservation of immunoreactivity and fine structure of adult *C. elegans* tissues using high-pressure freezing. *J. Histochem. Cytochem.* *52*, 1–12.
- Silacci, P., Mazzolai, L., Gauci, C., Stergiopulos, N., Yin, H.L., and Hayoz, D. (2004). Gelsolin superfamily proteins: key regulators of cellular functions. *Cell. Mol. Life Sci.* *61*, 2614–2623.
- Springer, J.E., Azbill, R.D., and Knapp, P.E. (1999). Activation of the caspase-3 apoptotic cascade in traumatic spinal cord injury. *Nat. Med.* *5*, 943–946.
- Stigloher, C., Zhan, H., Zhen, M., Richmond, J., and Bessereau, J.L. (2011). The presynaptic dense projection of the *Caenorhabditis elegans* cholinergic neuromuscular junction localizes synaptic vesicles at the active zone through SYD-2/liprin and UNC-10/RIM-dependent interactions. *J. Neurosci.* *31*, 4388–4396.
- Sulston, J.E. (1983). Neuronal cell lineages in the nematode *Caenorhabditis elegans*. *Cold Spring Harb. Symp. Quant. Biol.* *48*, 443–452.
- Thompson, W. (1983). Synapse elimination in neonatal rat muscle is sensitive to pattern of muscle use. *Nature* *302*, 614–616.
- Thompson, W.J. (1985). Activity and synapse elimination at the neuromuscular junction. *Cell. Mol. Neurobiol.* *5*, 167–182.
- Walsh, M.K., and Lichtman, J.W. (2003). In vivo time-lapse imaging of synaptic takeover associated with naturally occurring synapse elimination. *Neuron* *37*, 67–73.
- Wang, J.T., Medress, Z.A., and Barres, B.A. (2012). Axon degeneration: molecular mechanisms of a self-destruction pathway. *J. Cell Biol.* *196*, 7–18.
- Wang, J.Y., Chen, F., Fu, X.Q., Ding, C.S., Zhou, L., Zhang, X.H., and Luo, Z.G. (2014). Caspase-3 cleavage of dishevelled induces elimination of postsynaptic structures. *Dev. Cell* *28*, 670–684.
- White, J.G., Albertson, D.G., and Anness, M.A. (1978). Connectivity changes in a class of motoneurone during the development of a nematode. *Nature* *271*, 764–766.
- White, J.G., Southgate, E., Thomson, J.N., and Brenner, S. (1986). The structure of the nervous system of the nematode *Caenorhabditis elegans*. *Philos. Trans. R. Soc. Lond. B Biol. Sci.* *314*, 1–340.
- Williams, D.W., Kondo, S., Krzyzanowska, A., Hiromi, Y., and Truman, J.W. (2006). Local caspase activity directs engulfment of dendrites during pruning. *Nat. Neurosci.* *9*, 1234–1236.
- Yeh, E., Kawano, T., Weimer, R.M., Bessereau, J.L., and Zhen, M. (2005). Identification of genes involved in synaptogenesis using a fluorescent active zone marker in *Caenorhabditis elegans*. *J. Neurosci.* *25*, 3833–3841.
- Yeh, E., Kawano, T., Ng, S., Fetter, R., Hung, W., Wang, Y., and Zhen, M. (2009). *Caenorhabditis elegans* innexins regulate active zone differentiation. *J. Neurosci.* *29*, 5207–5217.
- Yuan, J., and Horvitz, H.R. (1992). The *Caenorhabditis elegans* cell death gene *ced-4* encodes a novel protein and is expressed during the period of extensive programmed cell death. *Development* *116*, 309–320.
- Yuan, J., Shaham, S., Ledoux, S., Ellis, H.M., and Horvitz, H.R. (1993). The *C. elegans* cell death gene *ced-3* encodes a protein similar to mammalian interleukin-1 beta-converting enzyme. *Cell* *75*, 641–652.
- Zhang, W., and Benson, D.L. (2001). Stages of synapse development defined by dependence on F-actin. *J. Neurosci.* *21*, 5169–5181.
- Zhang, Q.H., Chen, Q., Kang, J.R., Liu, C., Dong, N., Zhu, X.M., Sheng, Z.Y., and Yao, Y.M. (2011). Treatment with gelsolin reduces brain inflammation and apoptotic signaling in mice following thermal injury. *J. Neuroinflammation* *8*, 118.
- Zhang, Q.H., Li, J.C., Dong, N., Tang, L.M., Zhu, X.M., Sheng, Z.Y., and Yao, Y.M. (2013). Burn injury induces gelsolin expression and cleavage in the brain of mice. *Neuroscience* *228*, 60–72.
- Zhen, M., and Jin, Y. (1999). The liprin protein SYD-2 regulates the differentiation of presynaptic termini in *C. elegans*. *Nature* *401*, 371–375.
- Zhou, Q., Homma, K.J., and Poo, M.M. (2004). Shrinkage of dendritic spines associated with long-term depression of hippocampal synapses. *Neuron* *44*, 749–757.
- Zuo, Y., Lin, A., Chang, P., and Gan, W.B. (2005a). Development of long-term dendritic spine stability in diverse regions of cerebral cortex. *Neuron* *46*, 181–189.
- Zuo, Y., Yang, G., Kwon, E., and Gan, W.B. (2005b). Long-term sensory deprivation prevents dendritic spine loss in primary somatosensory cortex. *Nature* *436*, 261–265.